Available online at www.sciencedirect.com
ScienceDirect
Mendeleev Commun., 2012, **22**, 15–17
Mendeleev Communications

Rational design and synthesis of new PARP1 inhibitors

Leonid V. Romashov,[a] Alexey A. Zeifman,[b] Alexandra L. Zakharenko,[c] Fedor N. Novikov,[b] Viktor S. Stroilov,[b] Oleg V. Stroganov,[b] Germes G. Chilov,[b] Svetlana N. Khodyreva,[c] Olga I. Lavrik,[c] Ilya Yu. Titov[a,b] and Igor V. Svitan'ko*[a,b]

[a] *Higher Chemical College, Russian Academy of Sciences, 125047 Moscow, Russian Federation*
[b] *N. D. Zelinsky Institute of Organic Chemistry, Russian Academy of Sciences, 119991 Moscow, Russian Federation. Fax: +7 499 135 5328; e-mail: svitanko@mail.ru*
[c] *Novosibirsk Institute of Chemical Biology and Fundamental Medicine, Siberian Branch of the Russian Academy of Sciences, 630090 Novosibirsk, Russian Federation*

DOI: 10.1016/j.mencom.2012.01.005

A preliminary simulation of bioactive compounds followed by their synthesis have been carried out: a set of new fragment PARP1 inhibitors – 3,5,6,7-tetrahydro-4*H*-cyclopenta[4,5]thieno[2,3-*d*]pyrimidin-4-one derivatives – have been obtained. Molecular simulation has shown that binding is characterized by correlated hydrogen bonds with PARP1 and displacement of the highly-conservative water molecule by a polar group.

The poly(ADP-ribose)-polymerase-1 (PARP1) enzyme, which is localized in the cell nucleus, catalyzes the poly-ADP- ribosylation of proteins.[1] NAD^+ acts as an ADP-ribose donor. The PARP1-catalysed covalent modification regulates the activity of proteins involved in the regeneration of DNA damages and the maintenance of genome stability, gene transcription, proliferation and differentiation of cells, and other processes.[2,3] Thus, PARP1 inhibition, which is required to suppress the reparation and survival mechanisms of cells in the course of chemo- and radiotherapy, is considered a promising strategy for the treatment of cancer. The prevention of necrosis caused by a decrease in NAD^+ resources, which occurs in myocardial infarction and other pathophysiological states, is yet another therapeutic application of PARP inhibitors.[4] Finally, the inhibition of PARP1-stimulated transcription of proinflammatory genes can be beneficial in the therapy of cardiovascular diseases.[1] Previously, eight PARP1 inhibitors underwent clinical trials as both monotherapy agents and combinations with other antitumor agents.[5] However, the safety of prolonged use of these compounds has not been confirmed, so a need arises to create a broad range of new PARP1 inhibitors.

In this work, we used a high-performance virtual screening of a fragment library to find new PARP1 inhibitors. Fragment screening is a new paradigm for rational drug design, where the strongest binding fragments are first selected from a library of low-molecular-weight compounds with MW 150–300, and then the binding affinity is enhanced by linking or appending additional fragments.[6,7]

A fragment **1**, which is most strongly bound to PARP1, was selected during virtual screening. The computed pose [Figure 1(*a*)] is characterized by correlated hydrogen bonds between the carbonyl and NH groups of the pyrimidone ring and the G863 residue. The G863 residue is conservative in various PARP isoforms and PARPs from various species; it belongs to the set of structural filters describing the enzyme active site.[8] In addition to correlated hydrogen bonds, the tricyclic system of the compound interacted *via* π-stacking with the Y896 and Y907 residues.

As a result of the simulation based on active fragment **1**, it was suggested to synthesize structures **2**–**6**, which, according to the calculations, would show enhanced inhibiting activity for PARP1. In particular, molecular docking shows that the cyclopentane fragment of base compound **1** is bound in the pocket, which is formed by two hydrophobic residues Y896 and Y907,

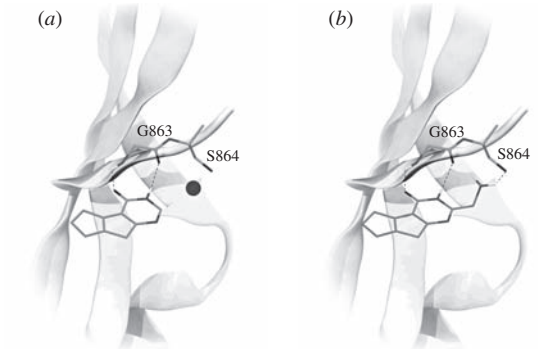

Figure 1 (*a*) Binding of compound **1** in the PARP1 active site according to simulation results. The water molecule is shown as a black sphere. (*b*) Binding of compound **6** with PARP1.

on its one side, and by charged residues E928 and K843, on the other. According to the results of the simulation, compound **2**, in which the five-membered ring is replaced with a six-membered one, has a larger area of hydrophobic contact with the enzyme; hence, it is bound more strongly at the active site.

Analysis of known PARP structures with various inhibitors has shown that the binding of a water molecule occurs near the main pharmacophoric group binding site. The major role in water binding belongs to hydrogen bonds with the G863 and S864 residues, while the spatial deviation of oxygen atoms is as small as 0.5 Å, suggesting a comparatively narrow localization of the molecule. It is known that similar conservative binding positions of water molecules play a very important role in protein–ligand binding;[9] hence, they should be taken into account in a rational design of inhibitors. Depending on the protein environment and the nature of the replacing group, the displacement of conservative water molecules may result in both a ligand affinity improvement due to a gain in entropy and energy losses. According to molecular docking results, the alkyl substituents in compounds **3**–**6** displace the water molecule from the conservative position; hence, according to computation results, their binding with PARP1 occurs more strongly than that of base fragment **1**.

Based on molecular simulation hypotheses, compounds **1**–**6** (Scheme 1)† were synthesized and the dose-dependent half maximal inhibitory concentrations for PARP1 (IC_{50}) were determined for them.‡ The three-stage syntheses of compounds **1** and **2** were carried

© 2012 Mendeleev Communications. All rights reserved.

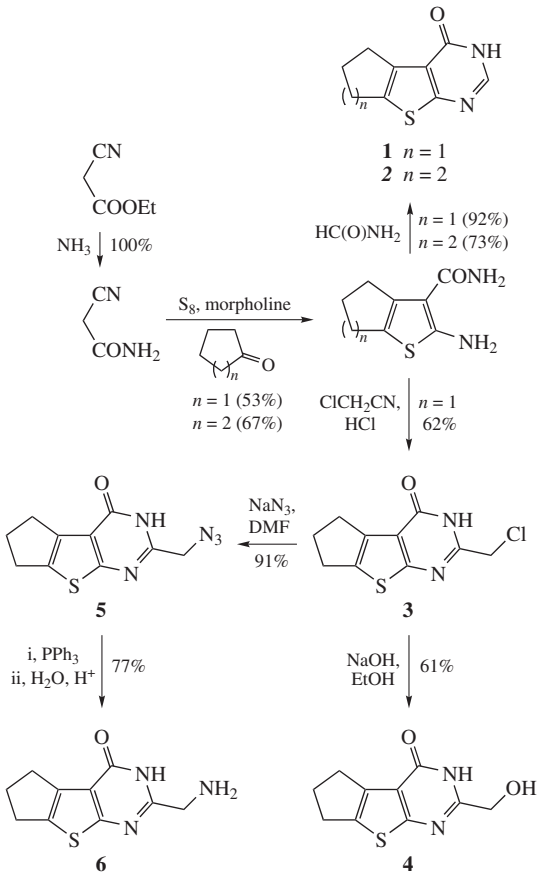

Scheme 1 Synthesis of compounds **1**–**6**.

out using published procedures.[10,11] The procedures used for synthesizing compounds **3**–**6** were described elsewhere.[12–15] Table 1 summarizes the inhibiting effects of the synthesized compounds. According to IC_{50} measurements, the efficiency of compound **2** (IC_{50} 160 μM, 95% confidence interval of 141–181 μM) is considerably lower than that of reference compound **1** (IC_{50} 17 μM, 95% confidence interval of 6–39 μM). IC_{50} measurements (Table 1) have shown that the displacement of conservative water apparently does not result in significant changes in the binding energy.

A comparison of the inhibition constants[§] of the compounds synthesized with the well-known data for PARP1 inhibitors

Table 1 New PARP1 inhibitors.

Substance	IC_{50}[a]/μM	K_i[b]/μM
1	16 (6; 39)	1.21
2	160 (141; 181)	12.3
3	47 (no data)	3.6
4	27 (18; 42)	2.1
5	26 (8; 92)	2.0
6	12 (6; 24)	0.9

[a] Experimental IC_{50} values (the numbers in parentheses show the confidence interval for 95% probability). [b] Experimental K_i values, calculated from IC_{50}.

(Figure 2) reveals that the new compounds are comparable to benzamide and quinazoline base fragments in binding affinity, which confirms the efficiency of a preliminary simulation in the organic synthesis of bioactive compounds.

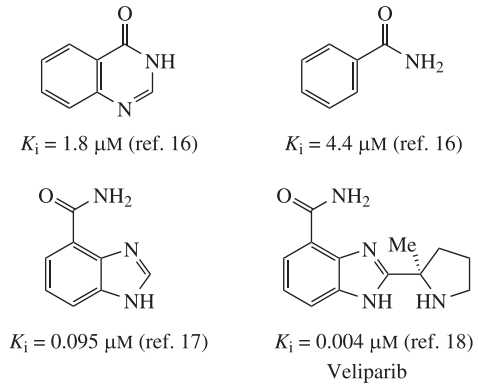

Figure 2

† *3,5,6,7-Tetrahydro-4*H*-cyclopenta[4,5]thieno[2,3-*d*]pyrimidin-4-one* **1**: mp 162–163 °C. ^{1}H NMR (500 MHz, DMSO-d_6) δ: 2.38 (q, 2H, CH_2, *J* 7.1 Hz), 2.91 (t, 4H, CH_2, *J* 7.1 Hz), 8.00 (s, 1H, CH), 12.39 (br.s, 1H, NH).

*5,6,7,8-Tetrahydro[1]benzothieno[2,3-*d*]pyrimidin-4(3*H*)-one* **2**, mp 164–165 °C. ^{1}H NMR (500 MHz, DMSO-d_6) δ: 1.77 (m, 4H, CH_2), 2.73 (br.s, 2H, CH_2), 2.87 (br.s, 2H, CH_2), 7.99 (s, 1H, CH), 12.29 (br.s, 1H, NH).

*2-(Chloromethyl)-3,5,6,7-tetrahydro-4*H*-cyclopenta[4,5]thieno[2,3-*d*]-pyrimidin-4-one* **3**: mp 159–161 °C. ^{1}H NMR (500 MHz, DMSO-d_6) δ: 2.30 (q, 2H, CH_2, *J* 7.1 Hz), 2.68 (t, 4H, CH_2, *J* 7.1 Hz), 3.66 (s, 2H, CH_2).

*2-(Hydroxymethyl)-3,5,6,7-tetrahydro-4*H*-cyclopenta[4,5]thieno-[2,3-*d*]pyrimidin-4-one* **4**: mp 129–133 °C. ^{1}H NMR (500 MHz, DMSO-d_6) δ: 2.38 (q, 2H, CH_2, *J* 7.2 Hz), 2.90 (t, 4H, CH_2, *J* 7.2 Hz), 4.36 (s, 2H, CH_2), 5.43 (br.s, 1H, OH), 12.02 (s, 1H, NH).

*2-(Azidomethyl)-3,5,6,7-tetrahydro-4*H*-cyclopenta[4,5]thieno[2,3-*d*]-pyrimidin-4-one* **5**: mp 140–143 °C. ^{1}H NMR (500 MHz, DMSO-d_6) δ: 2.37 (q, 2H, CH_2, *J* 7.1 Hz), 2.90 (t, 4H, CH_2, *J* 7.1 Hz), 3.41 (s, 2H, CH_2), 12.77 (s, 1H, NH).

*2-(Aminomethyl)-3,5,6,7-tetrahydro-4*H*-cyclopenta[4,5]thieno[2,3-*d*]-pyrimidin-4-one* **6**: mp 132–135 °C. ^{1}H NMR (500 MHz, DMSO-d_6) δ: 2.38 (q, 2H, CH_2, *J* 7.2 Hz), 2.90 (t, 4H, CH_2, *J* 7.2 Hz), 3.61 (s, 2H, CH_2), 5.51 (br.s, 2H, NH_2), 12.41 (s, 1H, NH).

‡ *Virtual screening and docking procedure.* Ligand docking was carried out using the Lead Finder software, version 1.1.15,[19] with default configuration parameters. The full-atomic model of PARP1 was prepared using the Model Builder software supplied in the Lead Finder distribution package. The starting structure of PARP1 was obtained from Protein Database, PDB ID: 1UK0. The binding energies of the ligands were assessed using the dG-scoring function available in Lead Finder. Fragment screening was based on an STK library provided by VitasM, http://www.vitasmlab.com/. Compounds from the STK library were broken into fragments according to a published procedure.[20] Calculated inhibition constants for compounds **1**–**6** are 80, 27, 11, 20, 23 and 20 μM, respectively.

Experimental measurement of inhibition constants. Recombinant human enzyme PARP1 was purified according to a reported procedure.[21] PARP1 inhibition was measured as follows: samples (15 μl) containing 200 nM of purified PARP1 protein, 2 OU cm^{-3} DNAse I-activated calf thymus DNA, 600 μM NAD^+, 0.5 μCi [^{3}H]NAD^+, 10% DMSO and compounds of interest in various concentrations were incubated for 1 min at 37 °C in a buffer solution (50 mM Tris, pH 8.0, 20 mM $MgCl_2$, 150 mM NaCl, 7 mM β-mercaptoethanol). The reaction rate was linear during the first 20 min under these conditions. The reaction was terminated by transferring a 12 μl aliquot portion on Whatman 1 paper filters soaked in 5% trichloroacetic acid. The filters were washed three times with 150 ml of 5% trichloroacetic acid, which was then washed off with 90% ethanol, and the filters were dried. The degree of inclusion of [^{3}H]ADP-ribose into an acid-insoluble material was measured with a QuantaSmart scintillation counter in a toluene scintillator. IC_{50} values were calculated using the Origin Pro 8.0 software by means of nonlinear regression analysis. All experiments were carried out in duplicate.

§ *Calculation of inhibition constants from IC_{50}.* IC_{50} values were converted to K_i using the competitive inhibition equation

$$K_i = IC_{50}/(1 + [NAD^+]/Km),$$

where $[NAD^+]$ is the NAD^+ concentration used in the experiments, and Km is the Michaelis constant of the reaction (according to published data,[22] Km = 50 μM).

References

1 D. D'Amours, S. Desnoyers, I. D'Silva and G. G. Poirier, *Biochem. J.*, 1999, **342 (Pt 2)**, 249.
2 P. O. Hassa, S. S. Haenni, M. Elser and M. O. Hottiger, *Microbiol. Mol. Biol. Rev.*, 2006, **70**, 789.
3 P. O. Hassa and M. O. Hottiger, *Front. Biosci.*, 2008, **13**, 3046.
4 P. Pacher and C. Szabo, *Cardiovasc. Drug Rev.*, 2007, **25**, 235.
5 H. Calvert and A. Azzariti, *Ann. Oncol.*, 2011, **22 Suppl 1**, i53.
6 F. N. Novikov and G. G. Chilov, *Mendeleev Commun*., 2009, **19**, 237.
7 V. S. Stroylov, T. V. Rakitina, F. N. Novikov, O. V. Stroganov, G. G. Chilov and A. V. Lipkin, *Mendeleev Commun*., 2010, **20**, 263.
8 F. N. Novikov, V. S. Stroylov, O. V. Stroganov, V. Kulkov and G. G. Chilov, *J. Mol. Model.*, 2009, **15**, 1337.
9 J. Luccarelli, J. Michel, J. Tirado-Rives and W. L. Jorgensen, *J. Chem. Theory Comput.*, 2010, **6**, 3850.
10 K. Gewald, E. Schinke and H. Böttcher, *Chem. Ber.*, 1966, **99**, 94.
11 B. R. Baker, R. E. Schaub, J. P. Joseph, F. J. McEvoy and J. H. Williams, *J. Org. Chem.*, 1952, **17**, 149.
12 S. Kanwar and S. D. Sharma, *Indian J. Chem., Sect. B*, 2005, **44**, 2367.
13 C. J. Shishoo, K. S. Jain, I. S. Rathod, B. J. Thakkar, S. B. Brahmbhatt, T. P. Gandhi, R. Bangaru and R. K. Goyal, *Arzneim.-Forsch.*, 1996, **46**, 273.
14 M. A. Ameen, S. Karsten and J. Liebscher, *Tetrahedron*, 2010, **66**, 2141.
15 D. Dhanak, S. D. Knight, P.-P. Lu, D. J. J. Morgans and B. C. Yao, WO 2003/103575, 2003.
16 M. Banasik, H. Komura, M. Shimoyama and K. Ueda, *J. Biol. Chem*., 1992, **267**, 1569.
17 A. W. White, R. Almassy, A. H. Calvert, N. J. Curtin, R. J. Griffin, Z. Hostomsky, K. Maegley, D. R. Newell, S. Srinivasan and B. T. Golding, *J. Med. Chem.*, 2000, **43**, 4084.
18 C. K. Donawho, Y. Luo, T. D. Penning, J. L. Bauch, J. J. Bouska, V. D. Bontcheva-Diaz, B. F. Cox, T. L. DeWeese, L. E. Dillehay, D. C. Ferguson, N. S. Ghoreishi-Haack, D. R. Grimm, R. Guan, E. K. Han, R. R. Holley-Shanks, B. Hristov, K. B. Idler, K. Jarvis, E. F. Johnson, L. R. Kleinberg, V. Klinghofer, L. M. Lasko, X. Liu, K. C. Marsh, T. P. McGonigal, J. A. Meulbroek, A. M. Olson, J. P. Palma, L. E. Rodriguez, Y. Shi, J. A. Stavropoulos, A. C. Tsurutani, G. D. Zhu, S. H. Rosenberg, V. L. Giranda and D. J. Frost, *Clin. Cancer Res.*, 2007, **13**, 2728.
19 O. V. Stroganov, F. N. Novikov, V. S. Stroylov, V. Kulkov and G. G. Chilov, *J. Chem. Inf. Model.*, 2008, **48**, 2371.
20 A. A. Zeifman, V. S. Stroylov, F. N. Novikov, O. V. Stroganov, A. L. Zakharenko, S. N. Khodyreva, O. I. Lavrik and G. G. Chilov, *J. Mol. Model.*, 2011, doi:10.1007/s00894-011-1280-4.
21 M. V. Sukhanova, S. N. Khodyreva and O. I. Lavrik, *Biokhimiya*, 2004, **69**, 686 [*Biochemistry (Moscow)*, 2004, **69**, 558].
22 F. Simonin, O. Poch, M. Delarue and G. de Murcia, *J. Biol. Chem.*, 1993, **268**, 8529.

Received: 7th September 2011; Com. 11/3797